Synthesis and characterization of SBA-3, SBA-15, and SBA-1 nanostructured catalytic materials

Oscar A. Anunziata , Andrea R. Beltramone,
Maria L. Martínez, Lizandra López Belon

Available online at www.sciencedirect.com
ScienceDirect
Journal of Colloid and Interface Science 315 (2007) 184–190
JOURNAL OF Colloid and Interface Science
www.elsevier.com/locate/jcis

Synthesis and characterization of SBA-3, SBA-15, and SBA-1 nanostructured catalytic materials

Oscar A. Anunziata *, Andrea R. Beltramone, Maria L. Martínez, Lizandra López Belon

Grupo Fisicoquímica de Nuevos Materiales, CITeQ, Facultad Córdoba, Universidad Tecnológica Nacional, Maestro López y Cruz Roja Argentina, 5016 Córdoba, Argentina

Received 1 March 2007; accepted 19 June 2007

Available online 23 June 2007

Abstract

A highly ordered large pore mesoporous silica molecular sieve SBA-3, SBA-15, Al-SBA-15, and SBA-1, were developed and characterized by XRD, BET, FTIR, SEM, and NMR-MAS. The catalytic materials were synthesized using different raw materials and operation conditions. These materials contain a regular arrangement of uniform channels with diameters between 1.8 and 10 nm, high specific surface area and high specific pore volume. The designed methods were effective for the synthesis, presenting each mesostructured materials, patterns of XRD and other characteristics corresponding to the reported ones in literature. The new route employed to synthesize Al-SBA-15, generates a catalyst with only aluminum in tetrahedral form, according to the data of ^{27}Al NMR-MAS. However, several reports indicated that the coordination of the Al atoms changes below the Si/Al ratio of 45, presenting peaks corresponding to penta and hexa-coordinated aluminum, which are absent in our samples (Si/Al = 50 and 33).

Keywords: Synthesis; Characterization; SBA-3; SBA-15; Al-SBA-15; SBA-1

1. Introduction

Various MMS (mesoporous molecular sieves), i.e., SBA, HMS, and MSU have been synthesized using super molecular groups (self-assembly of surfactants, with copolymers of low and/or high molecular weight) or blocks [1]. The MMS that in addition, showed microporous in their structure can be separated in three [2]: (1) MMS ($P6m$) synthesized with the copolymer blocks as groups, i.e., SBA-15 synthesized with $PPO_{20}PEO_{70}PPO_{20}$ as groups [3–6] or silica type with ethylene polystyrene-Co-poly (oxide) [7]. The micro-pores formation is due to the partial obstruction of the PEO chains into the silica walls during the synthesis. This structure coexists with the mesoporous structure. (2) MMS (cubic) synthesized under acidic conditions: SBA-1, SBA-6, and SBA-16 [8]. Bimodal distribution of the pores is a characteristically structure of these samples. (3) MCM-41 synthesized by hydrothermal or sol–gel method [9,10] with micro-pores formation due to the partial rupture of the silica wall. The mesoporous molecular sieves like SBA-1 and SBA-3 were synthesized at room temperature under acidic conditions [11]. The method was similar to SBA-15, except a low molecular weight quaternary alquilammonium template was used (i.e., QTA^+). SBA-3 (pore diameter >3 nm), SBA-1 (pore diameter >2 nm), can contain some micro-pores, too [12,13]. However, the micro-porosity is higher than SBA-15 [3], but with similar thermal and hydrothermal resistance. For that reason the development of this material is interesting for the application in high temperature catalytic processes, reactivation with oxygen and redox deposition of metals at nano-metric scale. SBA-15 possesses big tubular channels up to 30 nm de diameter [14,15]. As SBA-15 possesses the greater thickness of the pores walls, the hydrothermal stability is much higher than MCM-41 [14]. Although some studies of the incorporation of Al [16,17] and Ti [18] in SBA-15, as active species, were performed, the information is limited about the use of SBA-15 as host for the catalytic active specie. Anyway, this material presents a high potential in catalytic applications. Moreover, it application as sensors and nano-reactors due to its three-dimensional mesostructure (3-D)

* Corresponding author. Fax: +54 351 469058.
E-mail address: oanunziata@scdt.frc.utn.edu.ar (O.A. Anunziata).

0021-9797/$ – see front matter
doi:10.1016/j.jcis.2007.06.033

was developed, recently [19,20]. Pure siliceous materials have electrically neutral framework and consequently no Brönsted acidity. However, it is very difficult to prepare SBA-15 containing heteroatoms in the framework because of the strong acidic synthesis conditions. Recently, many efforts have been made to incorporate Al, Ti, and V into the framework of SBA-15, by post-synthesis grafting procedures [17,21,22] and direct synthesis [23,24]. The post-synthesis method always needs a complex experimental condition and the metal oxides tend to appear in the channels or external surface of the catalysts, which would block the channels [25]. Yue et al. tried to incorporate aluminum directly into the framework of SBA-15 through direct synthesis, but the product contains extra framework aluminum species and post-synthetic method is necessary to remove the extra framework aluminum [23].

In this work we report our first results of the development of SBA-3, SBA-15, Al-SBA-15, and SBA-1 mesoporous catalytic materials, characterized by XRD, BET, FTIR, SEM, and NMR-MAS.

2. Experimental

2.1. Synthesis

1. SBA-15 was synthesized using 15-Crown-15 (PEO15, Aldrich) as a co-polymer mono block and cetylpyridinium bromide, BDH 95% ($M_w = 402.47$) as surfactant. 15-Crown-15 (8 g) was added to an acid solution (50 ml of 37% HCl, in 200 ml of distilled water) at 50 °C for 6 h. A homogeneous solution was obtained; 17.5 g of TEOS at 50 °C with vigorous agitation were added, until complete hydrolysis (10 h) to final pH of 1. Finally, the surfactant (1.5 g) was added with continuous agitation at 0 °C, forming a dense gel in 30 min and pH 1.5, aging it at 90 °C during 72 h. The final product was filtered, washed and dried at 100 °C for 10 h. After, SBA-15 was immersed in ethanol reflux for 6 h, to extract the co-polymer block and the surfactant. Sample was filtered and washed with distilled water and dried at 100 °C and calcined at 550 °C in air for 6 h. A white powder, SBA-15 was obtained. In absence of cetylpyridinium bromide, SBA-15 is not obtained. To obtain the Al-SBA-15 the procedure was similar, at the moment of the addition of surfactant, 1.2–2.2 g of sodium aluminate was added, regulating the pH with HCl. The final Si/Al ratios were (a) 50 and (b) 33.

2. SBA-3 was prepared using cetyltrimethyl-ammonium bromide (CTMABr, Aldrich) and TEOS, Aldrich, el 98%, as a template and Si source, respectively. An aqueous solution of HCl (37%) was added in order to control the pH of the reaction system. 2 g of CTMABr and 40 ml de HCl (el 37%) were dissolved in 100 ml of water. TEOS (10 ml) was added dropping to the acidic solution of CTMABr with vigorous stirring at 30 °C. After 2 h, the white precipitated (SBA-3 mother) was aged at room temperature for 12 h. The sample was filtered and dried for 12 h at 100 °C. SBA-3 was immersed in ethanol reflux for 6 h, in order to extract the surfactant; after that, the sample was filtered and washed with distilled water. After drying it, SBA-3 was calcined at 550 °C in air for 8 h. The heating rate was 2 °C/min from 100 to 550 °C.

3. SBA-1 was synthesized using cetyltriethyl-ammonium bromide (CTEABr, Aldrich) as surfactant, distilled water and HCl, mixed to obtain a homogeneous system. This solution was cooled until 0 °C and stirred for 60 min. TEOS (Aldrich 98%) was added at 0 °C, under vigorous stirring. The molar composition of the reaction mixture was 0.11CTEABr, 1.2TEOS, 18HCl, 200H_2O. The mixture reacted at 0 °C under static conditions for 10 h. The resulting precipitated was filtered and washed with acetone, to facilitate the surfactant extraction. It was dried at 100 °C during 8 h, and calcined in air at 600 °C for 6 h, with a slope of 2 °C/min starting from 100 °C.

2.2. Characterization

The structure regularity of the samples was determined by XRD. JASCO 5300 FTIR spectrometer was used. The fingerprint of the samples were obtained using wafers of SBA in KBr. Acidity (for Al-SBA-15) was determined by FTIR of pyridine. A thermostatized cell with CaF_2 windows, warmed up to 400 °C and 4.2×10^{-2} Torr during 2 h was employed. Pyridine was adsorbed (5 Torr) at 25 °C for 10 h, and desorbed for 1 h at different temperatures and 10^{-3} Torr. The size and shape of the crystals were determined by SEM in a PHILIPS-SEM 501B. BET results were performed in ASAP 2010 equipment. ^{27}Al MAS NMR spectra were recorded at room temperature on a Bruker MSL-300 spectrometer with a resonance frequency of 78.21 MHz. The magnetic field was 7.05 Torr. The spin rate of the sample was 4.0 kHz and the number of scans was 4000–5000. The pulse lengths were adjusted to 4.6 μs with a repetition time of 500 ms. The sweep width was 29477 Hz, $AlCl_3 \cdot 6H_2O$ was used as a reference.

2.3. Catalytic activity

The catalytic decomposition of 2-propanol was used as a test reaction for the study of the acidity of SBA-15 and Al-SBA-15. A fixed bed tubular glass reactor working at atmospheric pressure was used, with a catalyst charge of 30 mg without dilution (0.2–0.3 mm particle size). Samples were pretreated at 200 °C in a N_2 flow for 3 h (60 ml/min). 2-propanol l was fed into the reactor by flowing N_2. None of the samples showed diffusion restrictions. The reaction products were analyzed by an on-line gas chromatograph provided with a FID detector and a fused silica capillary column.

3. Results and discussion

3.1. XRD and BET

The XRD patterns and BET results are shown in Table 1 and Figs. 1–3. The results are in agreement with literature data for materials synthesized by conventional methods [2,3,7].

Crystalline structure: the XRD patterns of the samples are shown in Figs. 1, 2, and 3, SBA-1, SBA-3, and SBA-15, respec-

Table 1
Textural and structural properties of the calcined samples

Sample	a_0[a] (nm)	Si/Al	Area (m^2/g)	Pore volume (ml/g)	Diameter[b] pore (nm)	Wall thickness[c] (nm)
SBA-1[d]	2.4	–	1520	0.71	2.4	–
SBA-3	3.6	–	1430	0.98	2.6	1.0
SBA-15	10.0	–	1040	1.38	8.9	1.1
Al-SBA-15(a)	11.3	50	1020	1.32	9.1	2.2
Al-SBA-15(b)	11.7	32	960	1.26	9.3	2.4

[a] Hexagonal: $a_0 = 2d_{100}/\sqrt{3}$.
[b] $D \cong 4V/A$.
[c] $E = a_0 - D$ (according Ref. [30]).
[d] Cubic: $a_0 = \sqrt{5}d_{210}$-cage diameter = 4.3, determined by using the equation of $D_{me} = a_0(6\varepsilon_{me}/\pi\nu)^{1/3}$. D_{me}: the cage diameter of a cubic unit cell of length a_0, ε_{me}: volume fraction of a regular cavity and ν ($\nu = 8$, for the SBA-1) is the number of cavities present in the unit cell [31].

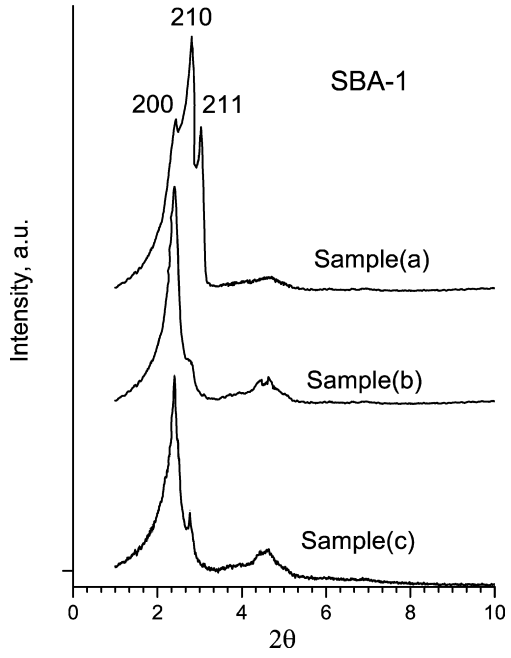

Fig. 1. XRD pattern of SBA-1. XRD patterns of as-synthesized SBA-1 mesoporous silica at 0 °C (samples a and c) and 20 °C (sample b), for synthesis molar composition: 0.11CTEABr, 1.2TEOS, 18HCl, 200H_2O (samples a and b); 0.09CTEABr:1.5TEOS:9HCl:125H_2O (sample c).

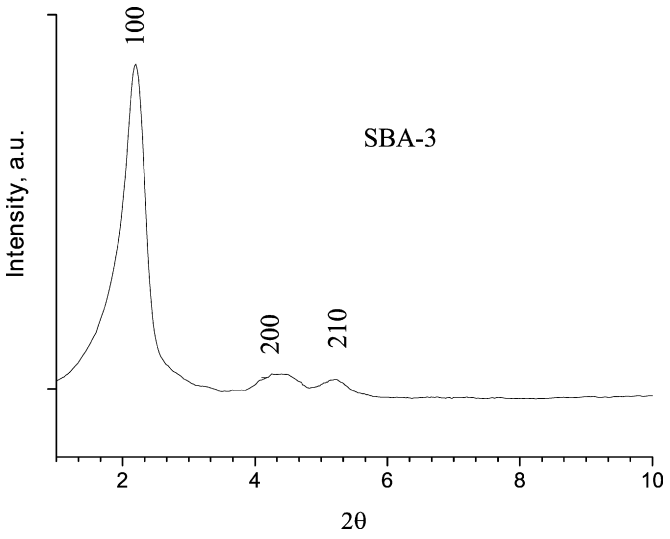

Fig. 2. XRD pattern of SBA-3.

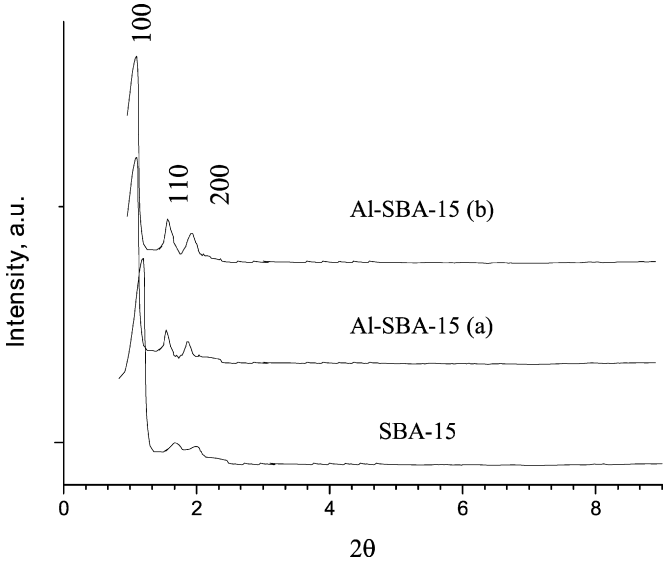

Fig. 3. XRD pattern of: SBA-15; Al-SBA-15a; and Al-SBA-15b.

tively. The pattern diffraction peaks confirm a high crystallinity (or long-range order structure in all samples).

In Fig. 1, we can observe signals at 2.3°, 2.6°, and 3° (2θ), corresponding at 200, 210, and 211 (hkl) index reflections based on the SBA-1 mesoporous silica of $Pm3n$ cubic mesostructure, as was reported in literature for pure cubic SBA-1, but in this case, using another synthesis way [10,26]. Thus, according the surfactant used in the preparation of SBA-1 (CTEABr), the lower reaction temperature and the ratio of surfactant/Si, we obtain a pure cubic phase of SBA-1 at very short reaction time using different Si source and pH value, compared with a recent work of Man-Chien Chao et al. [26]. The mesoporous materials formation was explained in terms of self-assembly surfactants in a solution to guide the formation of the inorganic precursor via condensation reactions.

Reports were made [27] in which shown that the morphology was easier to control under acid conditions because the interaction between the surfactant and silica framework is weaker than the alkaline route.

Large head-group surfactants such as C_n TABr ($n = 12$, 14, 16, 18) favors the SBA-1 cubic $Pm3n$ phase, It is well known that liquid crystal phases of surfactants, are heavily dependent on temperature. The kinetics of the hydrolysis of TEOS followed by condensation/polymerization is also highly dependent on temperature. The temperature of the reaction system therefore would be a key factor in determining the structure and morphology of mesoporous materials [27,28]. In conclusion, as a function of experimental results showed in Fig. 1, the structural mesophases order gradually decreases with the temperature increases or the ratio CTEABr/Si decreases. This aspect may be underlined.

The surfactant packing parameter, g, given by $g = V/(a_0 l)$, where V is the total volume of the surfactant chain, a_0 is the

effective head group area at the organic–inorganic interface, and l is the surfactant chain length, is considered to be a useful molecular structure-directing index to characterize the geometry of the mesophase products, and can be used to rationalize the above XRD results. At low synthesis temperatures, e.g., at 0 and 20 °C, the large head group surfactant CTEABr effectively stabilizes a more curved surface ($g < 1/3$) for the formation of cubic SBA-1. With increasing the synthesis temperature, however, the conformational disorder due to the surfactant tail motion increases the effective surfactant volume, leading to a corresponding increase in the g value. This situation results in a phase change from cubic to hexagonal mesophase ($1/3 < g < 1/2$).

When the synthesis temperature is superior to 20 °C, the surfactant exhibits a hexagonal adjustment SBA-3 [26], the low hydrolysis of the TEOS gives as result a more flexible silica network and a selection of hexagonal phase SBA-3 happens to 30 °C. Therefore, the phase determination into cubic SBA-1 or hexagonal SBA-3 is also influenced by the charge density matching between the silicate and surfactant micelles. The usual synthesis of SBA-1 is based on the $S^+X^-I^+$ pathway, where S^+ denotes the cationic surfactant, X^- the acid anion, and I^+ the inorganic (silica) species, under strongly acidic conditions and low synthesis temperatures, but longer reaction time [29], than we employed in this work with high successfully.

The Miller indexes 100, 200 and 210 corresponding to 2.3°, 4.3°, and 5.2° (2θ) for hexagonal SBA-3 [10] can be observed in Fig. 2. In the case of SBA-15, the main signal appears at 1.2° (2θ) and shifts to lower angles with the incorporation of Al to 0.9° (2θ) for sample Al-SBA-15, with higher content of Al (see Table 1), as we expected, comparing with literature data [2,3].

3.2. FTIR

FTIR of Si-SBA-15 and Al-SBA-15 (Fig. 4) shows bands at 1069 cm^{-1} (T–O asymmetric stretching) and 800 cm^{-1} (T–O symmetric stretching). The bands are due to TO_4 vibrations (T = Si, Al), assigned to the bending Al–O–Si, that indicate the incorporation of Al into SBA-15 [32,33]. Only one signal at 3740 cm^{-1} due to terminal Si–OH is observed in the case of SBA-15; a new band at 3630 cm^{-1} appears in Al-SBA-15, increasing from sample (a) to (b), assigned to Brönsted sites due Si_3–O–Al–OH. SBA-3 shows only a band at 3647 cm^{-1}, due to terminal silanol. A band at 3720 cm^{-1} for SBA-1 indicates a weaker acid site compared with SBA-3 and SBA-15.

Various works determine the density and strength of acid sites of different AlSBA-15 by temperature-programmed-desorption (TPD) of ammonia [34,35] or pyridine [36], without differentiating Brönsted to Lewis sites. Recently, acidic properties of Al-SBA-15 materials prepared by post-synthesis alumination mesoporous silica, were determined by FTIR of Pyridine [37,38]. In our case, using FTIR of preadsorbed and desorbed pyridine at different temperatures (as it were indicated in Section 2) we distinguish the presence of both sites, those that, in addition, are in correspondence with the later results of ^{27}Al NMR-MAS showed in the next section. Thus, the total acidity of sample (a) was 0.200, 0.178, and 0.1 mmol/g; for sample (b): 0.298, 0.210, and 0.185 mmol/g of Py retained at 250, 350, 400 °C, respectively. The Brönsted/Lewis ratio for the samples are: 12, 19, and 28 for sample a; 8, 12 and 13 for sample b, at 250, 350, and 400 °C respectively, see Figs. 5a and 5b.

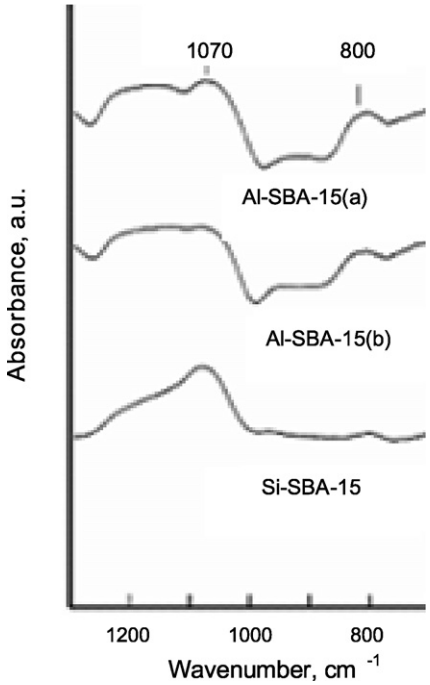

Fig. 4. FTIR of Si-SBA-15 and Al-SBA-15.

3.3. SEM

The size and shape of the samples indicate good morphology of the crystals, without other phases, and typical of these materials. The pictures are shown in Figs. 6a–6c.

As shown in Fig. 6, separated almost spherical or spheroid crystals but have glass-like disorder in the walls observed for SBA-1 sample. The particle size of the siliceous SBA-1 was 1.5–2.2 μm in diameter, whereas for SBA-3 the crystal form is almost spherulitic with lower crystal size (0.8–1.3 μm). SBA-15 images reveal that it consists of many rope-like domains with relatively uniform sizes of 1.5–2 μm, which are aggregated into wheat-like macrostructures (rod-like primary particles aggregate to form micron-sized fibers).

3.4. NMR-MAS

^{27}Al NMR-MAS results of the Al-SBA-15 samples are shown in Figs. 7a and 7b. Two peaks at 53 and 0 ppm were observed in sample b, although it's very lower. The chemical shift of ^{27}Al NMR-MAS at 53 ppm can be assigned to aluminum in tetrahedral form, in which the aluminum is incorporated into the siliceous wall. The chemical shift at 0 ppm is usually assigned to octahedral extra framework aluminum. Though, the incorporation efficiency decreases with the increase of the concentration of aluminum species, most Al exist in a tetrahedral envi-

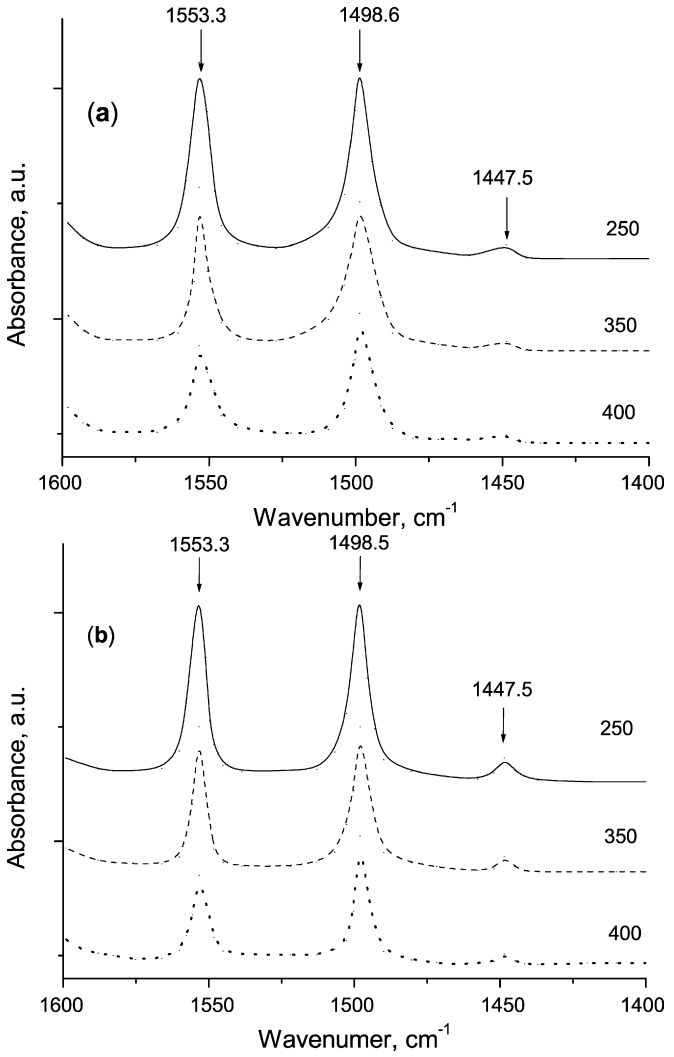

Fig. 5. FTIR spectra for the pyridine-adsorbed at room temperature and 10^{-3} Torr on Al-SBA-15a and Al-SBA-15b and desorbed at 250, 350, and 400 °C at 10^{-3} Torr for 1 h.

ronment. It is widely accepted that the coordination status of Al is directly related to its acidity. The hydroxyl groups linked to Al in tetrahedral coordination will produce Brönsted acidic sites, and by dehydroxylation at higher temperature, would give rise to Lewis sites, while octahedrally-coordinated aluminum does not impart Brönsted acidity. Thus, the procedure employed to synthesize Al-SBA-15 by a new route, generates a catalyst with aluminum only in tetrahedral form. However, in recent report [22–24], indicated that the coordination of the Al atoms is changed below the n_{Si}/n_{Al} ratio of 45. Al-SBA-15 (Si/Al = 7 or 23) shows a sharp peak centered around 53 ppm and two small peaks centered around 7 ppm and 22 ppm. The peaks corresponding to 22 and 7 ppm are attributed to penta- and hexa-coordinated aluminum which might have formed by leaching during calcination.

3.5. Catalytic activity

Isopropanol conversion and 1-butene isomerization are often applied as catalytic tests to obtain the effective catalytic

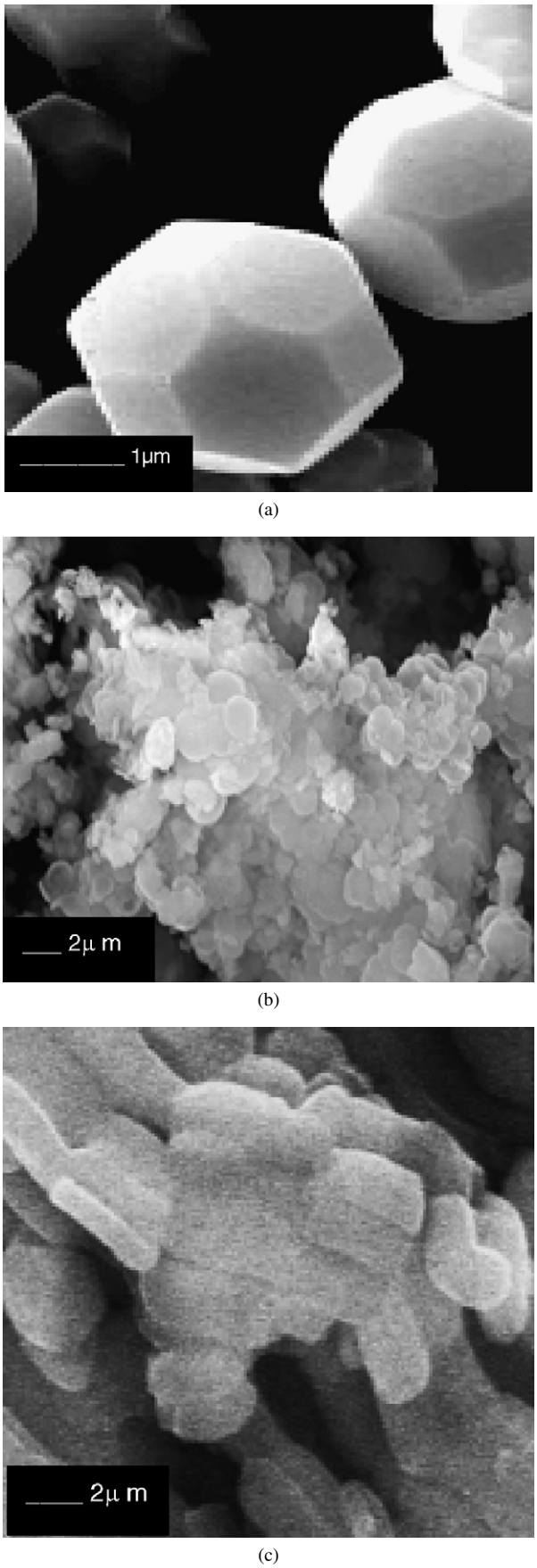

Fig. 6. SEM microphotographs of (a) SBA-1, (b) SBA-3, and (c) SBA-15.

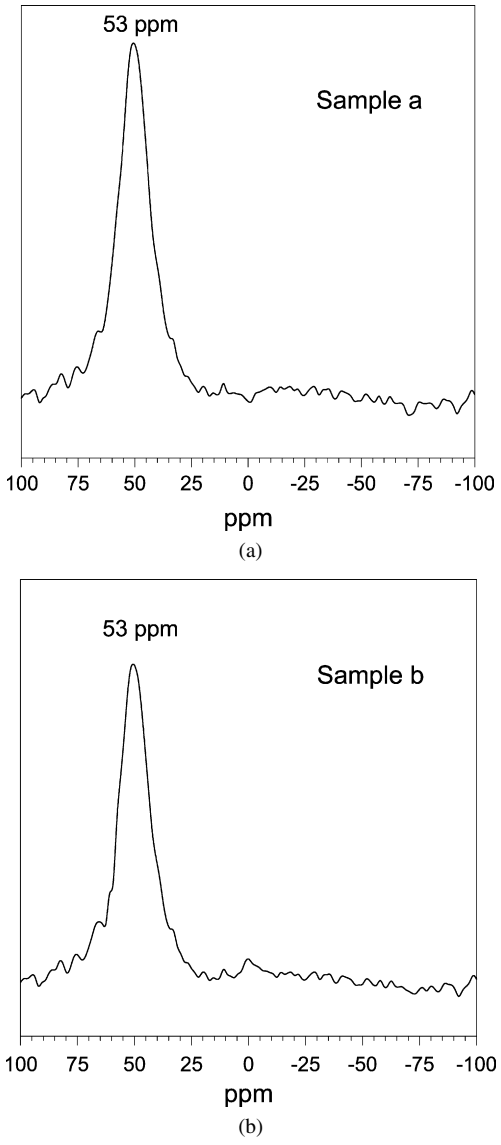

Fig. 7. (a) ^{27}Al MAS NMR spectra of Al-SBA-15a. (b) ^{27}Al MAS NMR spectra of Al-SBA-15b.

properties of acid centers. Thus, in the isopropanol conversion, catalysts can be classified according to their degree of acidity in dehydration or the dehydrogenation of propene or acetone, respectively. The dehydration of isopropanol to propylene takes place on acid sites, whereas dehyrogenation to acetone is accomplished on redox or basic sites.

The conversions obtained at different temperatures are compiled in Fig. 8. Whilst Si-SBA-15 is not active in this reaction (at 200 °C, 2.1% conversion), the aluminum-containing SBA-15, exhibits very high conversion at this temperature (100% conversion). When the reaction is carried out at a lower temperature (175 °C), different conversions appear for these materials as a function of the aluminum content. The conversion is higher for the Al-32-SBA-15 at all reaction temperature. For higher Al contents an increase in the conversion takes place. The selectivity was close to 100% for propene for all the Al_x-SBA-15 materials at any reaction temperature.

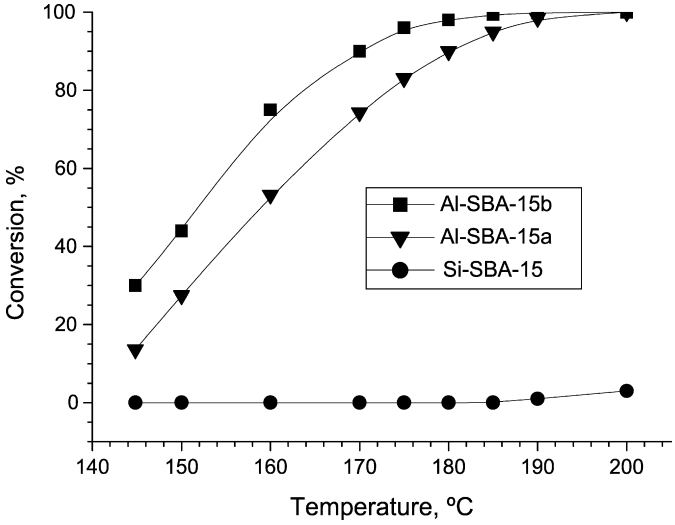

Fig. 8. Catalytic activity of Si and Al-SBA-15 for 2-propanol. Al-SBA-15a: (Si/Al = 50); Al-SBA-15b: (Si/Al = 32); Si-SBA-15.

4. Conclusions

SBA-1, SBA-3, and SBA-15 and Al-SBA-15, were developed successfully. The designed methods were effective for the synthesis. The materials have good structural and textural properties. SBA-1 showed only cubic phase. SBA-15 was prepared employing two surfactants cetylpyridinium bromide and a co-polymer mono block, 15-Crown-15. Al-SBA-15 does not contain extra framework aluminum species as was indicated by NMR-MAS. The catalytic properties of Al-SBA-15 for 2-propanol dehydration, indicated that acid center are only the active sites within the Al-SBA-15 mesostructure. Is noticeable the increasing in the wall thickness in the case of Al-SBA-15 compared to SBA-15, conferring to the material a higher thermal and hydrothermal resistance.

Acknowledgments

O.A.A. and A.R.B., Conicet Researcher, M.L.M., Conicet Fellowship, L.L.B., Foncyt Fellowship. This work was supported by CONICET Argentina, PIP No. 6394 (2005–2007) and FONCYT PICT No. 14-14448 (2005–2008).

References

[1] F.X. Chen, X.D. Huang, Q.Z. Li, Chin. Sci. Bull. 44 (1999) 1905.
[2] F. Chen, X. Jun Xu, S. Shen, S. Kawi, K. Hidajat, Micropor. Mesopor. Mater. 75 (2004) 231.
[3] R. Ryoo, C.H. Ko, M. Kruk, V. Antochshuk, M. Jaroniec, J. Phys. Chem. B 104 (2000) 11465.
[4] B.L. Newalkar, S. Komarneni, Chem. Mater. 13 (2001) 4573.
[5] A. Galarneau, H. Cambon, F.D. Renzo, F. Fajula, Langmuir 17 (2001) 8328.
[6] C.-M. Yang, B. Zibrowius, W. Schmidt, F. Schüth, Chem. Mater. 15 (2003) 3739.
[7] C.G. Goltner, B. Smarsly, B. Berton, M. Antonietti, Chem. Mater. 13 (2001) 1617.
[8] Y. Sakamoto, M. Kaneda, O. Terasaki, D.Y. Zhao, J.M. Kim, G. Stucky, H.J. Shin, R. Ryoo, Nature 408 (2000) 449.

[9] A. Sayari, P. Liu, M. Kruk, M. Jaroniec, Chem. Mater. 9 (1997) 2499.
[10] A. Sayari, M. Kruk, M. Jaroniec, Catal. Lett. 49 (1997) 147.
[11] Q. Huo, D. Margolese, G.D. Stucky, Chem. Mater. 8 (1996) 1147.
[12] P.A. Albouy, A. Ayral, Chem. Mater. 14 (2002) 3391.
[13] J.-S. Lee, S.H. Joo, R. Ryoo, J. Am. Chem. Soc. 124 (2002) 1156.
[14] E. Zhao, J. Feng, Q. Huo, N. Melosh, G.H. Fredrickson, B.F. Chmelka, G.D. Stucky, Science 279 (1998) 548.
[15] E. Zhao, Q. Huo, J. Feng, B.F. Chmelka, G.D. Stucky, J. Am. Chem. Soc. 120 (1998) 6024.
[16] M. Cheng, Z. Wang, K. Sakurai, F. Kumat, T. Saito, T. Komatsu, T. Yashima, Chem. Lett. (1999) 131.
[17] Z. Luan, M. Hartmann, D. Zhao, W. Zhou, L. Kevan, Chem. Mater. 11 (1999) 1621.
[18] Z. Luan, E.M. Maes, P.A.W. van der Heide, D. Zhao, R.S. Czernuszewicz, L. Kevan, Chem. Mater. 11 (1999) 3680.
[19] M.S. Morey, A. Davidson, G.D. Stucky, J. Porous Mater. 5 (1998) 195.
[20] R. Ryoo, S. Jun, J.M. Kim, M.J. Kim, Chem. Commun. (1997) 2225.
[21] M.S. Morey, S. O'Brien, S. Schwarz, G.D. Stucky, Chem. Mater. 12 (2000) 898.
[22] Z. Luan, J.Y. Bae, C. Kevan, Chem. Mater. 12 (2000) 3202.
[23] Y. Yue, A. Gedeon, J.L. Bonardet, N. Melosh, J.B. D'Espinose, J. Fraissard, Chem. Commun. (1999) 1697.
[24] L.N. Bharat, O. Johnson, K. Sridhar, Chem. Mater. 13 (2001) 552.
[25] R. Murugavel, H.W. Roesky, Angew. Chem. Int. Ed. Engl. 109 (1997) 4491.
[26] M.C. Chao, H. Ping Lin, D.S. Wang, C.Y. Tang, Micropor. Mesopor. Mater. 83 (2005) 269.
[27] S. Che, Y. Sakamoto, O. Terasaki, T. Tatsumi, Micropor. Mesopor. Mater. 85 (2005) 207.
[28] P. Srinivasu, S. Hyun Lim, Y. Kubota, T. Tatsumi, Catal. Today 111 (2006) 379.
[29] H.-M. Kao, C.C. Cheng, Mater. Lett. 60 (2006) 2594.
[30] F. Chen, A. Shen, X.-J. Xu, R. Xu, F. Kooli, Micropor. Mesopor. Mater. 79 (2005) 85.
[31] A. Vinu, V. Murugesan, M. Hartmann, Chem. Mater. 15 (2003) 1385.
[32] A. Corma, C. Corell, V. Fornes, W. Kolodziejski, J. Perez-Pariente, J. Catal. 15 (1995) 576.
[33] M. Janicke, C. Landry, S. Christiansen, S. Britalan, G. Stucky, B. Chmelka, Chem. Mater. 11 (1999) 1342.
[34] A. Gédéon, A. Lassoued, J.L. Bonardet, J. Fraissard, Micropor. Mesopor. Mater. 44–45 (2001) 801.
[35] A. Vinu, G. Satish Kumar, K. Ariga, V. Murugesan, J. Mol. Catal. A Chem. 235 (2005) 57.
[36] G. Chandrasekar, M. Hartmann, M. Palanichamy, V. Murugesan, Catal. Commun. 8 (2007) 457.
[37] M. Gómez-Cazalilla, J.M. Mérida-Robles, A. Gurbani, E. Rodríguez-Castellón, A. Jiménez-López, J. Solid State Chem., doi: 10.1016/j.jssc.2006.12.038.
[38] Y.-S. Ooi, S. Bhatia, Micropor. Mesopor. Mater., doi: 10.1016/j.micromeso.2006.12.044.